Toxicogenomic differentiation of functional responses to fipronil and imidacloprid in *Daphnia magna*

Julia Pfaff, Hannes Reinwald, Steve U. Ayobahan, Julia Alvincz, Bernd Göckener, Orr Shomroni, Gabriela Salinas, Rolf-Alexander Düring, Christoph Schäfers and Sebastian Eilebrecht

Supplemental material

Supplemental material and methods

Transcriptomics

For transcriptome analysis, only RNA samples with a 28S/18S ratio > 2.0 were used. Sequencing libraries were prepared for each sample from 100 ng/µl total RNA at the sequencing facility "NGS-Services for Integrative Genomics" at the University of Göttingen in Germany. According to their standard workflow, Poly(A)+ RNA was purified from total RNA samples and subjected to cDNA library preparation using the TruSeq RNA Library Prep Kit v2 as recommended by the manufacturer (Illumina, San Diego, USA). Libraries were validated using a Fragment Analyzer system (Agilent, Santa Clara, USA), before being sequenced on an Illumina HiSeq 4000 System (Illumina, San Diego, USA) in 50 bp single read mode, producing approximately 30 million raw reads per sample. Sequence images were transformed with Illumina software BaseCaller to BCL files, which was then demultiplexed to fastq files with bcl2fastq v2.17.1.14. Adapter sequences were removed using trimmomatic v0.39 (Bolger et al. 2014) and library's sequence quality was assessed with FastQC v0.11.5 (Andrews 2010). Sequences were aligned to the *Daphnia magna* reference genome (daphmag2.4, GCA_001632505.1), containing a total of 27.350 genes, using STAR v2.5.2a allowing for 2 mismatches within 50 bases (Dobin et al. 2013), resulting in alignment rates between 86.4% and 95.4%. Subsequently, feature mapped read counting was performed using featureCounts v1.5.0-p1 with default settings (Liao et al. 2014). Chromosomal coverage was assessed using samtools v1.10.2. Mapped read tables were merged to a single count matrix for each substance and analyzed via R v3.6.2 (R Core Team 2019) using RStudio v1.2.5033 (Loraine et al. 2015). All available package versions used in the analysis are listed in the R-session report file in the supplementary information. After removing low abundance gene counts (sum of counts across all samples < 9), differential gene expression analysis was conducted via DESeq2 v1.26.0 (Love et al. 2014) based on three biological replicates per condition. Gene counts were normalized using DESeq2's negative binomial distribution model, applying a parametric fit type to the dispersion estimate model. In cases where parametric fit type performed poorly a local fit type was implemented. Count outliers were identified and removed via Cook's distance with the default settings implemented in DESEq2's outlier detection. After GLM fitting, mean gene count values were subject to pairwise Wald's t-testing comparing each treatment to its respective control group. Resulting p-values were corrected for multiple testing following Benjamini-Hochberg with independent hypothesis weighting (IHW) (Ignatiadis et al. 2016). An effect size cut off (LFcut) was computed for each treatment as the 90% quantile of the absolute non-shrunk lfc values. This was done to account for the general lower effect size observed in the low exposure treatments. That way the effect size cutoff scales with the global effect size distribution, which varies with the exposure concentration. Then, apeglm effect size shrinking was applied to the original lfcs (Zhu et al. 2019). A transcript was considered as a differentially expressed gene (DEG) when padj < 0.05 and the absolute apeglm shrunk lfc was greater than the predefined LFcut. Raw reads (fastq) and processed data (raw and normalized gene count matrix) were deposited in the ArrayExpress database at EMBL-EBI (www.ebi.ac.uk/arrayexpress) (Athar et al. 2019) under accession numbers E-MTAB-9829 (fipronil) and E-MTAB-9830 (imidacloprid). The reviewer access is user name: Reviewer_E-MTAB-9829 password: cv2on5yz (fipronil) and user name: Reviewer_E-MTAB-9830 password: QH4QVvig (imidacloprid).

Chemical analysis

The concentrations of fipronil and imidacloprid in the aqueous samples were determined by chemical analysis that was performed separately for both substances by high performance liquid chromatography coupled with tandem mass spectrometry (HPLC–MS/MS).

For analysis of fipronil, samples of 1000 µL volume were diluted with 200 µL acetonitrile in autosampler vials. Where necessary, samples were priorly diluted with copper-free water to yield concentrations within the calibration range. Data were collected on a binary Waters 2695 HPLC system coupled to a Waters Micromass Quattro micro tandem mass spectrometer operated in negative electrospray ionization (ESI-) mode. Chromatographic separation was performed on a Phenomenex Gemini column (C18, 5 µm, 150 mm x 3 mm) at a flow rate of 0.5 mL/min and a column temperature of 30 °C. The injection volume was 10 µL.

The following mobile phases (MP) were used: 2 mM ammonium acetate in methanol (MP A) and 2 mM ammonium acetate in water/methanol (90/10, v/v, MP B). The following linear gradient program was applied: 0 – 0.1 min: 30% MP A, 70% MP B; 2.5 – 5.4 min: 100% MP A, 0% MP B; 5.5 – 8.0 min: 30% MP A, 70% MP B. The mass transition used for the quantification of fipronil was m/z 434.9 > m/z 329.9; the confirmation of the substance's identity was carried out via the mass transitions m/z 434.9 > m/z 250.0 and m/z 434.9 > m/z 317.9.

A seven-point matrix calibration with copper-free water and acetonitrile levels was used in a concentration range from 0.15 µg/L to 25 µg/L (referring to the aqueous part). The coefficient of determination (r^2) of the linear calibration function was determined to be >0.99. The analytical method was successfully validated for copper-free water on two fortification levels (0.5 and 20 µg/L) according to the EU guideline SANCO/3029/991 at a limit of quantification (LOQ) of 0.5 µg/L. The accuracy (overall mean recovery) was 97.5% and the precision was 2.5% (RSD of the recovery values). Two quality control (QC) samples with concentrations of 1.0 and 12 µg/L were used for the ongoing verification of the matrix calibration. Recoveries of QC samples were within a range of 80 – 120%. Matrix-charged procedural blanks and controls were prepared and run with the samples to exclude possible cross-contaminations during laboratory work.

Chemical analysis of imidacloprid was conducted with a method similar as described above for fipronil. The substance specific differences are described in the following: All imidacloprid samples were diluted as described before, but 50 µL of an internal standard solution (50 mg/L d4-imidacloprid in acetonitrile) was added before measurement. The injection volume for HPLC-MS/MS analysis was reduced to 5 µL. For chromatographic separation of imidacloprid, the same mobile phases were used as for fipronil analysis. However, the linear gradient was slightly changed to the following parameters: 0 – 0.1 min: 10% MP A, 90% MP B; 2.8 – 5.4 min: 100% MP A, 0% MP B; 5.5 – 8.0 min: 10% MP A, 90% MP B. The mass spectrometer was operated in positive electrospray ionization mode (ESI+) and the following mass transitions were used for quantification of imidacloprid: m/z 256.1 > m/z 175.1 (quantifier) and m/z 256.1 > m/z 209.1 (qualifier). For d4-imidacloprid, the following mass transitions were used: m/z 260.1 > m/z 179.1 (quantifier) and m/z 260.1 > m/z 213.1. A matrix calibration with copper-free water and acetonitrile ranging from 30 – 3,000 µg imidacloprid/L (referring to the aqueous part) was used. The concentration of the internal standard was 250 µg/L (referring to the aqueous part) in each calibration solution. The method was successfully validated on two fortification levels (100 µg/L and 2,000 µg/L) and a resulting LOQ of 100 µg imidacloprid/L. The accuracy (overall mean recovery) was 100.0% and the precision was 1.0% (RSD of all recovery values). QC samples at levels of 200 and 2,000 µg/L were used and showed recoveries within the acceptable range of 80 – 120%. Matrix-charged procedural blanks were found to be free of quantifiable traces of imidacloprid.

Supplemental tables

Table S 1: Analytical parameters of the tap water used to conduct the modified Acute Immobilization Test with *D. magna.*

analytical parameter		value
conductivity (µS/cm)		256.0
NO_3 (mg/L)		6
NO_2 (mg/L)		< 0.005
NH_4 (mg/L)		< 0.01
PO_4 (mg/L)		0.24
total hardness °d (mmol/L)		5.60 (1.0)
alkalinity (mmol/L)		1.8
calcium hardness °d (mmol/L)		5.04 (0.9)
magnesium hardness °d (mmol/L)		0.56 (0.1)
non-purgeable organic carbon (mg/L)		0.6260
Cd (µg/L)		0.006
Cr (µg/L)		0.073
Cu (µg/L)		1.233
Fe (µg/L)		0.184
Mn (µg/L)		0.070
Ni (µg/L)		0.180
Pb (µg/L)		0.014
Zn (µg/L)		4.32
Chlorine (mg/L)	total	0.03
	free	< 0.02
	bound	< 0.01

Table S 2: BLASTX results for the DEGs of the fipronil-specific signature in *D. magna* (see **Figure 1**). Lfc = $\log_2$-fold change after exposure to the HE of fipronil.

Ensembl gene ID	protein hit	query coverage [%]	identity [%]	E value	organism	lfc	annotation
APZ42_002042	cuticle protein 21-like	55	98	8.00E-04	Daphnia magna	1.10	cuticle
APZ42_004806	uncharacterized protein	80	100	2.00E-21	Daphnia magna	-3.91	unknown
APZ42_010553	larval cuticle protein 65Ag1-like	97	99.01	1.00E-65	Daphnia magna	-3.80	cuticle
APZ42_010953	coiled-coil domain containing protein 9-like isoform X3	36	38.46	4.00E-13	Daphnia magna	-1.93	architecture of organelles
APZ42_011063	keratin-associated protein 19-2-like	25	100	5.00E-04	Daphnia magna	-3.77	cuticle
APZ42_012100	putative C-type lectin domain family 2 member D3	99	100	0.00E+00	Daphnia magna	-1.76	immune defense
APZ42_012777	repretitive proline-rich cell wall protein 1-like	40	100	8.00E-17	Daphnia magna	-2.95	architecture of organelles
APZ42_013500	uncharacterized protein	99	100	1.00E-08	Daphnia magna	-3.32	unknown
APZ42_013866	endocuticle structural glycoprotein SgAbd-3-like	99	100	1.00E-99	Daphnia magna	-3.20	cuticle
APZ42_014254	keratin-associated protein 21-1-like isoform X2	27	80.85	7.00E-05	Daphnia magna	-2.40	cuticle
APZ42_014962	uncharacterized protein	98	100	4.00E-18	Daphnia magna	-1.96	unknown
APZ42_015038	spidroin-1-like	99	99.29	2.00E-64	Daphnia magna	-2.06	architecture of organelles
APZ42_015080	carbonic anhydrase 1	99	100	0.00E+00	Daphnia magna	-2.27	acid-based regulation
APZ42_015189	mitochondrial substrate carrier family protein U	27	59.09	0.032	Daphnia magna	-1.73	transport
APZ42_015755	uncharacterized protein	99	100	0.00E+00	Daphnia magna	-2.67	unknown
APZ42_015769	YHT domain-containing protein 1-like	74	95.7	1.00E-15	Daphnia magna	-2.09	gene expression regulation
APZ42_015798	SEC14-like protein 2	99	100	0.00E+00	Daphnia magna	-1.04	lipid metabolism

APZ42_015799	cytochrome p450 26A1	96	100	0.00E+00	Daphnia magna	1.96	gene expression regulation
APZ42_016356	deleted in malignant brain tumors 1 protein-like	67	34.55	2.00E-42	Pseunomyrmex	-2.01	immune defense
APZ42_017067	no significant similarity found					-1.57	unknown
APZ42_017273	G-protein-coupled receptor Mth2	99	100	0.00E+00	Daphnia magna	-1.20	stress response
APZ42_017321	myosin-6-like isoform X1	95	100	0.00E+00	Daphnia magna	-1.49	transport
APZ42_017323	salivary gland secretion-like protein	99	100	0.00E+00	Daphnia magna	-1.45	digestion
APZ42_017452	putative C1q and tumor necrosis factor-related protein 3	99	43.85	6.00E-92	Daphnia magna	1.55	lipid metabolism
APZ42_017457	putative C1q and tumor necrosis factor-related protein 3	97	48.85	4.00E-93	Daphnia magna	1.20	lipid metabolism
APZ42_017532	ganglioside GM2 activator-like	98	59.3	3.00E-63	Daphnia magna	1.35	lipid metabolism
APZ42_017534	pro-resilin-like	72	99.19	2.00E-80	Daphnia magna	-2.06	movement
APZ42_017563	no significant similarity found					-3.22	unknown
APZ42_017566	no significant similarity found					-3.52	unknown
APZ42_017567	no significant similarity found					-3.18	unknown
APZ42_017570	uncharacterized protein	99	100	8.00E-161	Daphnia magna	-1.25	unknown
APZ42_018394	6-phosphogluconate dehydrogenase, decarboxylating	99	100	0.00E+00	Daphnia magna	-1.48	lipid metabolism
APZ42_018834	uncharacterized protein	99	100	0.00E+00	Daphnia magna	-1.90	unknown
APZ42_019444	maleless-like protein	99	100	0.00E+00	Daphnia magna	-1.10	RNA processing
APZ42_019827	chymotrypsin-2-like	93	100	0.00E+00	Daphnia magna	-5.42	digestion
APZ42_019883	uncharacterized protein	99	100	0.00E+00	Daphnia magna	-1.22	unknown
APZ42_020664	cuticular protein	99	100	2.00E-79	Daphnia magna	-2.54	cuticle
APZ42_021110	cuticular-like protein	78	100	2.00E-52	Daphnia magna	-3.96	cuticle

APZ42_021116	proline-rich protein 3-like	99	98.92	2.00E-88	Daphnia magna	-4.19	RNA processing
APZ42_021525	endocuticle structural glycoprotein SgAbd-1-like	91	100	8.00E-102	Daphnia magna	-2.98	cuticle
APZ42_022395	mucin-17-like	66	43.45	3.00E-28	Daphnia magna	1.51	movement
APZ42_022519	carbonic anhydrase 14	99	100	0.00E+00	Daphnia magna	-1.78	acid-based regulation
APZ42_022684	putative macrophae MHC class I receptor 2 protein	99	100	0.00E+00	Daphnia magna	-2.24	immune defense
APZ42_023119	putative Ccp84Ae	80	100	0.00E+00	Daphnia magna	-2.97	cuticle
APZ42_023136	repetitive proline-rich cell wall protein-like isoform X1	72	99.31	9.00E-135	Daphnia magna	-2.36	architecture of organelles
APZ42_023284	extensin-like	39	96.61	8.00E-42	Daphnia magna	-2.45	architecture of organelles
APZ42_023530	cell wall integrity and stress response component 4-like	88	71.11	8.00E-66	Daphnia magna	-1.94	architecture of organelles
APZ42_023533	cell wall integrity and stress response component 4-like	61	98.99	8.00E-96	Daphnia magna	-2.06	architecture of organelles
APZ42_023550	uncharacterized protein	99	100	0.00E+00	Daphnia magna	-1.58	unknown
APZ42_023954	putative dipeptidyl peptidase 1	99	100	0.00E+00	Daphnia magna	-2.53	digestion
APZ42_024006	putative defense protein 3	87	42.21	4.00E-26	Daphnia pulex	-1.56	immune defense
APZ42_024008	glucosamine-6-phosphate isomerase 2-like isoform X1	99	100	0.00E+00	Daphnia magna	-1.45	other
APZ42_024011	putative dipeptidyl peptidase 1	99	55.42	2.00E-117	Daphnia magna	-1.71	digestion
APZ42_024479	proline-rich extensin-like protein EPR1	77	99.2	3.00E-127	Daphnia magna	-1.49	architecture of organelles
APZ42_024553	4-aminobutyrate aminotransferase, mitochondrial	99	100	0.00E+00	Daphnia magna	-2.56	GABA catabolism
APZ42_026378	chorion peroxidase	99	100	0.00E+00	Daphnia magna	-2.73	other
APZ42_027347	cuticle protein CP14.6-like	99	95.93	2.00E-109	Daphnia magna	-3.56	cuticle
APZ42_027350	larval cuticle protein 65Ag1-like	99	100	1.00E-11	Daphnia magna	-4.05	cuticle

APZ42_028486	uncharacterized protein	98	100	5.00E-19	Daphnia magna	1.29	unknown
APZ42_029381	cuticle protein 3-like isoform X1	99	99.42	6.00E-96	Daphnia magna	-3.41	cuticle
APZ42_029383	cuticular protein 49Ag	89	100	0.00E+00	Daphnia magna	-3.41	cuticle
APZ42_029386	larval cuticle protein 65Ag1-like	99	100	2.00E-96	Daphnia magna	-3.03	cuticle
APZ42_029392	larval cuticle protein 65Ag1-like	99	100	2.00E-11	Daphnia magna	-2.88	cuticle
APZ42_029422	endocuticle structural glycoprotein SgAbd-1-like	99	98.94	2.00E-96	Daphnia magna	-4.12	cuticle
APZ42_029425	cuticle protein CP14.6-like	99	100	2.00E-99	Daphnia magna	-3.31	cuticle
APZ42_029440	endocuticle structural glycoprotein ABD-4-like isoform X2	99	99.4	1.00E-10	Daphnia magna	-2.75	cuticle
APZ42_029643	no significant similarity found					-2.80	unknown
APZ42_030380	uncharacterized protein	99	100	2.00E-76	Daphnia magna	-1.71	unknown
APZ42_031877	ATP-dependent RNA helicase glh-2-like	15	100	1.90E-02	Daphnia magna	-2.61	RNA processing
APZ42_031885	ATP-dependent RNA helicase glh-2-like	99	99.11	1.00E-16	Daphnia magna	-3.34	RNA processing
APZ42_032096	cuticle protein 1b	96	100	1.00E-05	Daphnia magna	-4.00	cuticle
APZ42_032408	phospholipase D1	90	100	0.00E+00	Daphnia magna	-1.15	lipid metabolism
APZ42_032551	glycine, alanine and asparagine-rich protein-like	6	100	1.00E-10	Daphnia magna	-2.03	other
APZ42_032711	uncharacterized protein	99	100	1.00E-161	Daphnia magna	-2.27	unknown
APZ42_033011	endochitinase	99	100	0.00E+00	Daphnia magna	-2.07	cuticle
APZ42_033092	carboxylesterase 3	99	100	0.00E+00	Daphnia magna	-1.28	lipid metabolism
APZ42_033872	uncharacterized protein	98	100	6.00E-51	Daphnia magna	-1.71	unknown
APZ42_033900	uncharacterized protein	91	100	2.00E-76	Daphnia magna	-2.13	unknown
APZ42_034176	putative class B basic helix-loop-helix protein	99	100	1.00E-13	Daphnia magna	-1.98	gene expression regulation

Table S 3: BLASTX results for the DEGs of the imidacloprid-specific signature in *D. magna* (see **Figure 2**). Lfc = log_2-fold change after exposure to the HE of imidacloprid.

Ensembl gene ID	protein hit	query coverage [%]	identity [%]	E value	organism	lfc	annotation
APZ42_004238	putative Aminopeptidase N	95	100	0.00E+00	Daphnia magna	-2.21	digestion
APZ42_008961	transmembrane protease serine 11D-like	74	86.5	1.00E-32	Daphnia magna	-2.52	immune defense
APZ42_011485	cyanophycinase-like	88	100	8.00E-18	Daphnia magna	6.98	other
APZ42_013491	Aminopeptidase N	99	100	0.00E+00	Daphnia magna	2.92	digestion
APZ42_014381	uncharacterized protein	23	100	6.00E-08	Daphnia magna	3.00	unknown
APZ42_014896	putative Aminopeptidase N	95	100	0.00E+00	Daphnia magna	5.46	digestion
APZ42_014897	Aminopeptidase N	99	100	2.00E-163	Daphnia magna	2.22	digestion
APZ42_015765	uncharacterized protein	99	98.1	0.00E+00	Daphnia magna	4.41	unknown
APZ42_015863	neuropeptide-like protein 31	27	92.3	7.00E-03	Daphnia magna	1.47	synaptic signaling
APZ42_017246	uncharacterized protein	98	100	3.00E-47	Daphnia magna	1.56	unknown
APZ42_020839	uncharacterized protein	98	100	3.00E-51	Daphnia magna	-1.36	unknown
APZ42_021087	mucin-2-like	80	98.98	4.00E-158	Daphnia magna	2.01	movement
APZ42_023946	ervatamin-B-like	99	98.5	0.00E+00	Daphnia magna	1.98	digestion
APZ42_024330	penicilin-binding transpeptidase	73	37.04	8.00E-03	uncultured bacterium	2.94	other
APZ42_024851	cysteine-rich protein	40	54.76	9.00E-10	Trametes coccinea	2.69	unknown
APZ42_028669	mucin-2-like isoform X1	77	99.66	1.00E-152	Daphnia magna	2.23	movement
APZ42_032074	uncharacterized protein	99	100	0.00E+00	Daphnia magna	2.94	unknown
APZ42_032082	acetylgalactoaminyl-O-glycosyl-glycoprotein	97	96.97	9.00E-88	Daphnia magna	1.02	movement
APZ42_033277	no significant similarity					3.45	unknown

Table S 4: BLASTX results for the DEGs of the overlap of imidacloprid- and fipronil-specific signatures in *D. magna* (see **Figure 3A**).

Ensembl gene ID	protein hit	query coverage [%]	identity [%]	E value	organism	annotation
APZ42_016017	transcriptional regulatory protein LGE1-like	99	100	7.00E-83	Daphnia magna	gene expression regulation
APZ42_019540	uncharacterized protein	98	100	4.00E-31	Daphnia magna	unknown
APZ42_022082	keratin-associated protein 19-2-like	41	98.33	1.00E-09	Daphnia magna	cuticle
APZ42_024268	C1q and tumor necrosis factor-related protein 3-like protein	93	43.05	6.00E-66	Daphnia magna	lipid metabolism
APZ42_024851	cysteine-rich protein	40	54.76	1.00E-09	Trametes coccinea	unknown
APZ42_028140	Dehydrogenase/reductase SDR family member 4	99	100	0.00E+00	Daphnia magna	retinoic acid metabolism
APZ42_028669	mucin-2-like isoform X1	77	99.66	1.00E-152	Daphnia magna	movement
APZ42_028799	Decaprenyl-diphosphate synthase subunit 2	99	100	0.00E+00	Daphnia magna	other
APZ42_032074	uncharacterized protein	99	100	0.00E+00	Daphnia magna	unknown

Supplemental figures

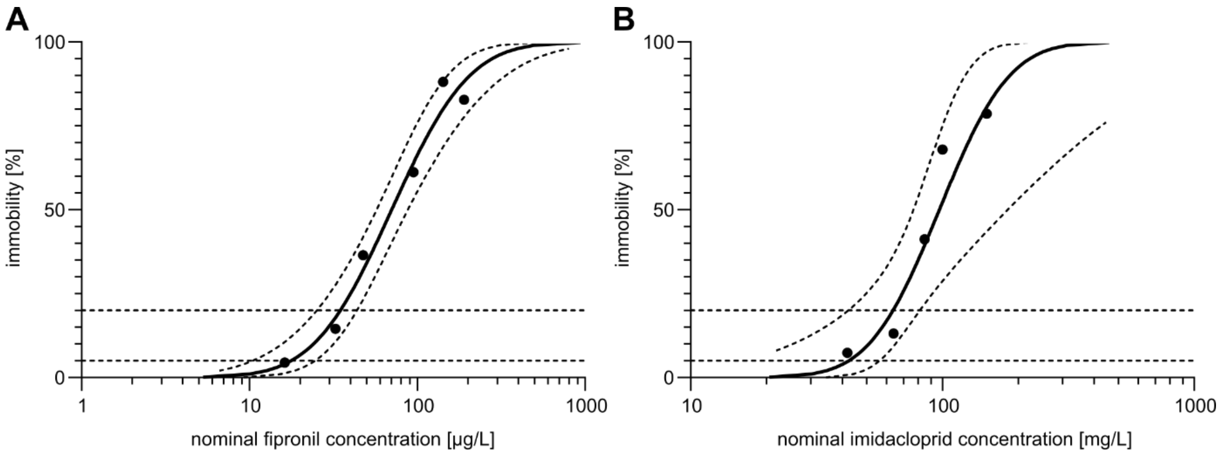

Figure S 1: Range finding exposure experiments for identifying low effect concentrations of fipronil and imidacloprid in the modified Acute Immobilization Test with *D. magna.* **(A)** Immobility [%] at 48 hours was plotted against the nominal concentration of fipronil. 95% confidence intervals are indicated as dotted lines. 5% and 20% effect levels are given as horizontal lines. **(B)** as (A), but for imidacloprid.

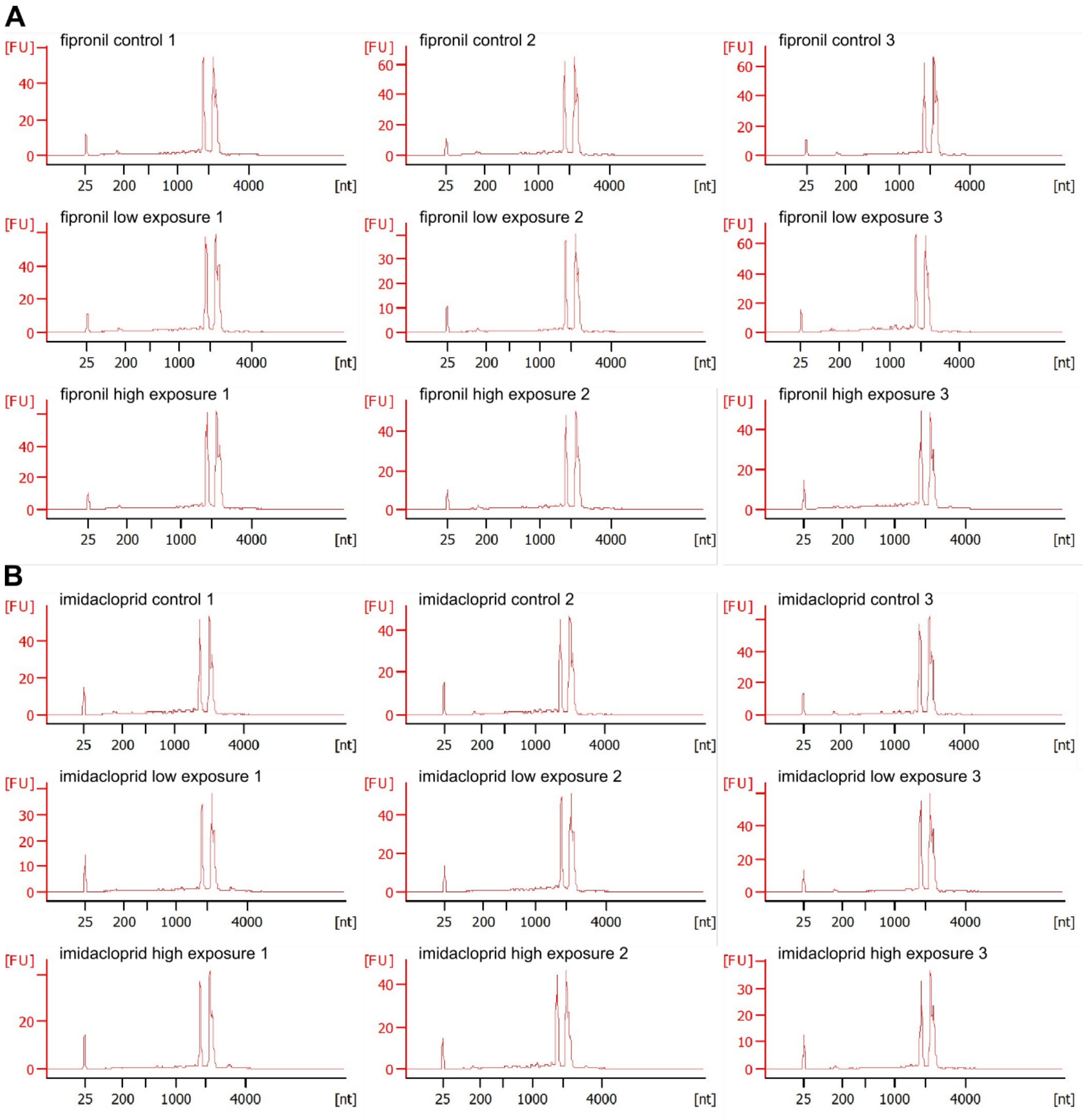

Figure S 2: 2100 Bioanalyzer electropherograms of the total RNA samples used for sequencing. **(A)** RNA profiles obtained for all three replicates of the exposure experiment with fipronil. Experimental conditions and replicate numbers are indicated. **(B)** as (A), but for the exposure experiment with imidacloprid.

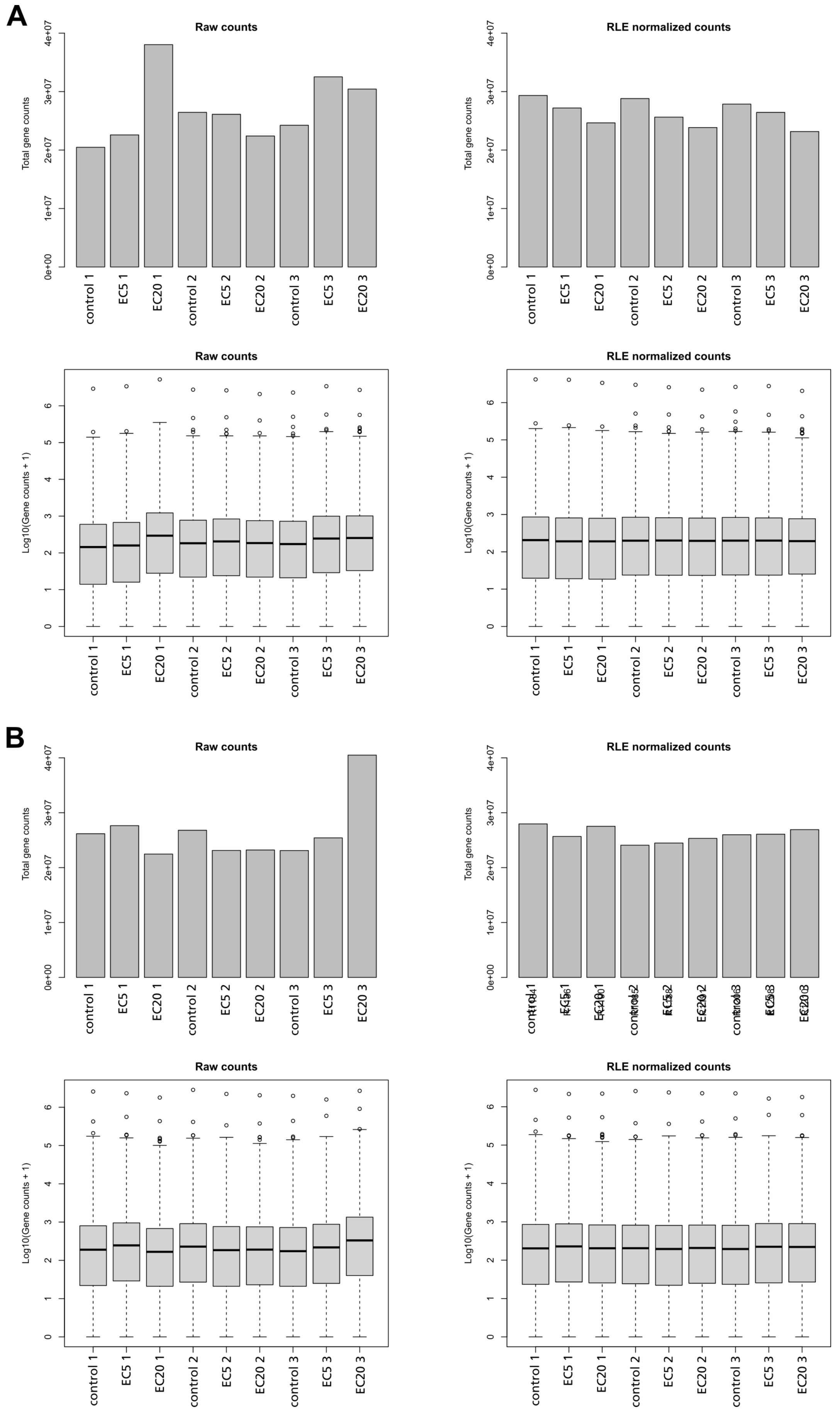
A
Raw counts
RLE normalized counts
Total gene counts
0e+00
1e+07
2e+07
3e+07
4e+07
Log10(Gene counts + 1)
control 1
EC5 1
EC20 1
control 2
EC5 2
EC20 2
control 3
EC5 3
EC20 3
B

Figure S 3: RNA-Seq read count normalization using DESeq2. **(A)** Raw (left) and Relative log Expression (RLE) normalized read counts of samples taken after exposure to the LE and the HE of fipronil as well as the corresponding controls. Biological replicates are numbered. **(B)** Raw (left) and Relative log Expression (RLE) normalized read counts of samples taken after exposure to the LE and the HE of imidacloprid as well as the corresponding controls. Biological replicates are numbered.

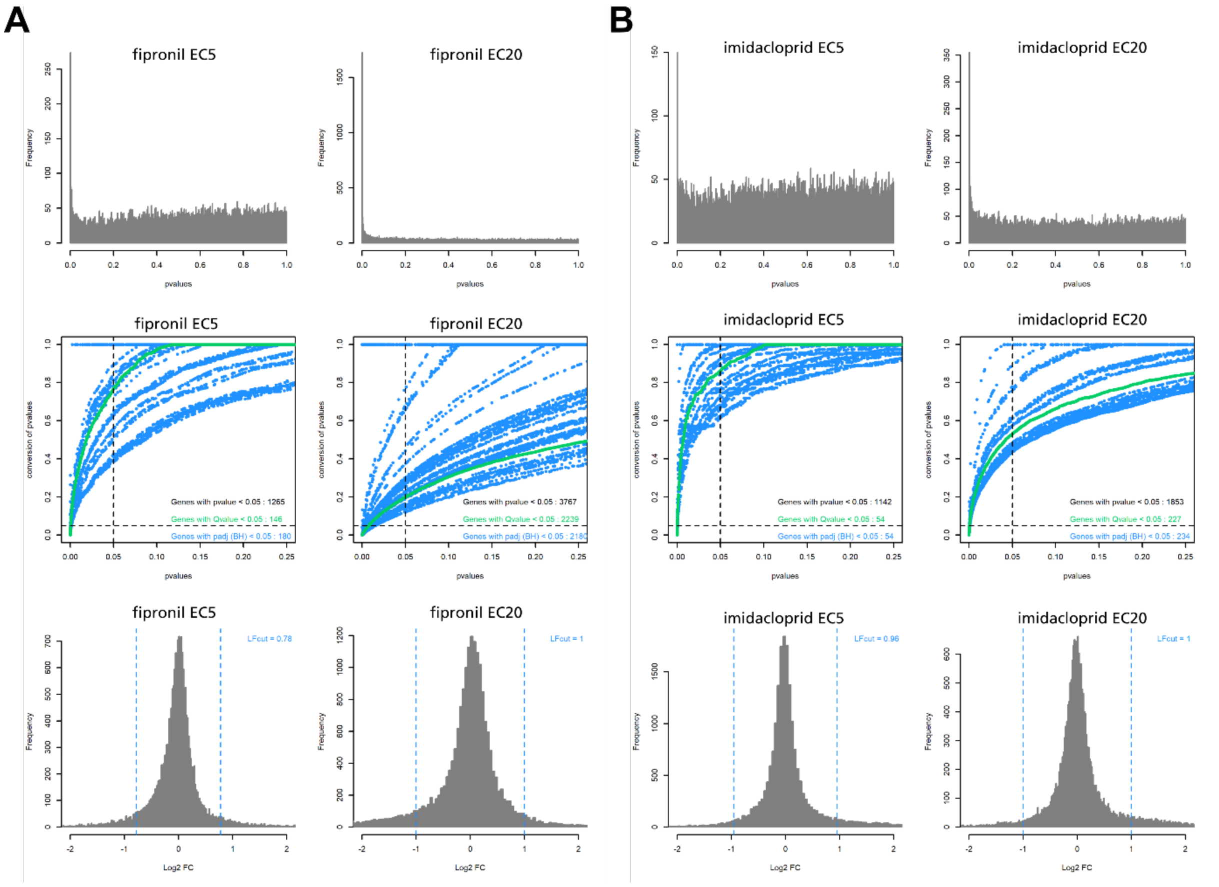

Figure S 4: Distributions of p-values, p-value conversion and log_2-fold change distributions after LE and HE exposure to fipronil and imidacloprid as observed by gene expression data compared to the control in pair wise fashion. **(A)** Distribution of p-values (Wald's t-test) of all genes after exposure to the LE and the HE of fipronil (left) and after exposure to the LE and the HE of imidacloprid (right). **(B)** Obtained Wald's p-values against converted p-values for multiple testing after Benjamini-Hochberg and respective p-values for exposure to the LE and the HE of fipronil (left) and after exposure to the LE and the HE of imidacloprid (right). Only genes with a p-value < 0.26 are displayed. **(C)** Distribution of log_2-fold change values of all genes after exposure to the LE and the HE of fipronil (left) and after exposure to the LE and the HE of imidacloprid (right). The log_2-fold change cut-off for each condition is given and indicated as a dotted line.

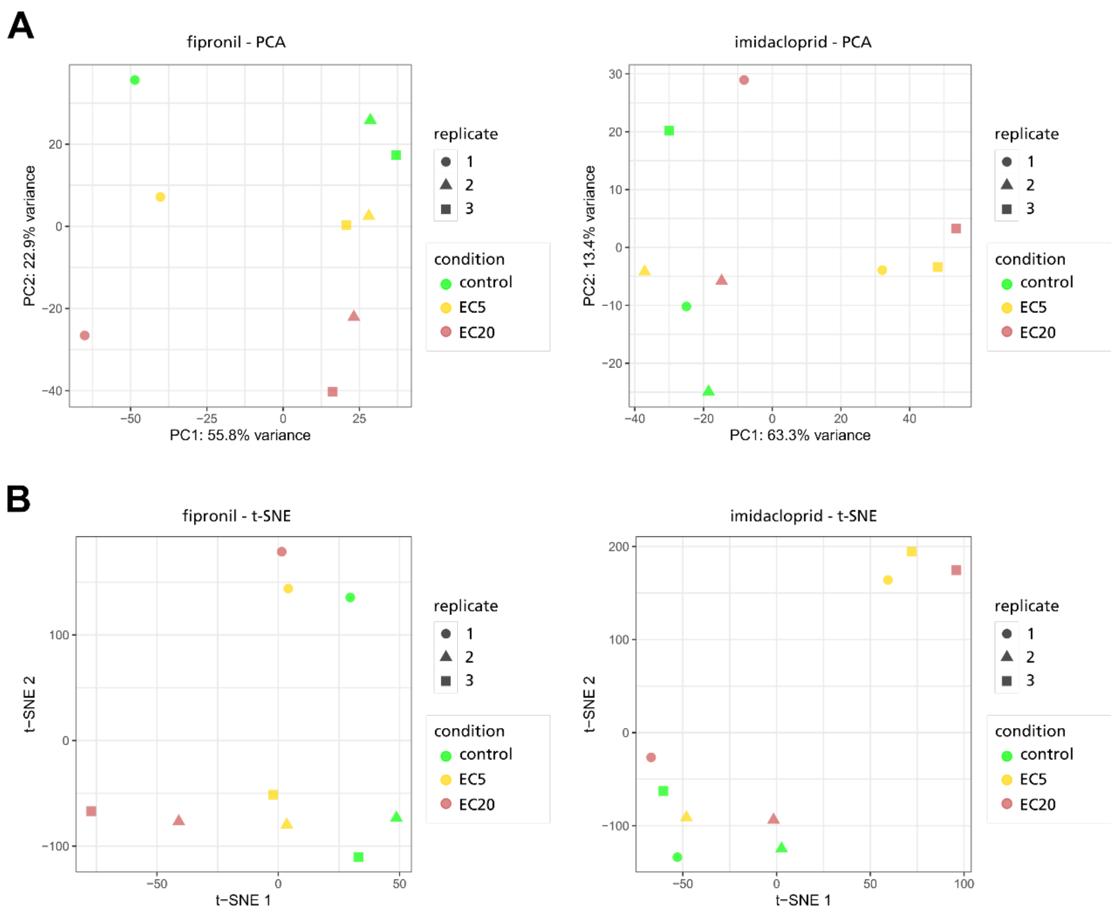

Figure S 5: Principle component analysis (PCA) and t-distributed stochastic neighbour embedding (t-SNE) of samples after exposure to the LE and the HE of fipronil and imidacloprid as observed by RNA-Seq. **(A)** PCA of control samples and samples after exposure to the LE and the HE of fipronil (left) and imidacloprid (right). Biological replicates are indicated as symbols, conditions are indicated as color code. **(B)** t-SNE of control samples and samples after exposure to the LE and the HE of fipronil (left) and imidacloprid (right). Biological replicates are indicated as symbols, conditions are indicated as color code.

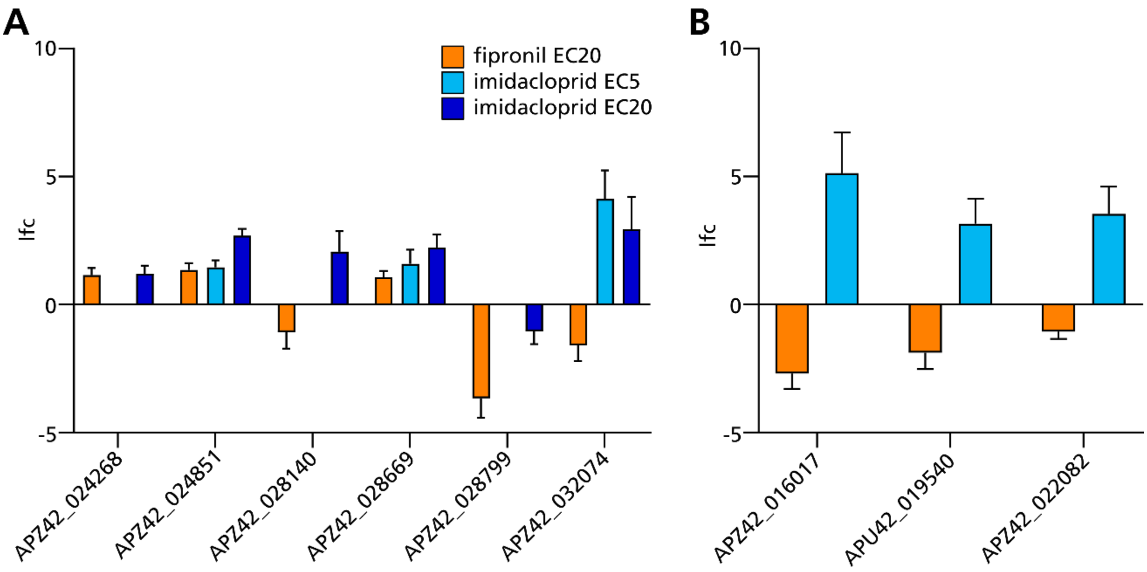

Figure S 6: Differential expression of all genes in the common subset of DEGs after exposure to fipronil and imidacloprid. **(A)** The $\log_2$-fold change (lfc) of the six genes in the common subset of DEGs after exposure to the HE of fipronil (orange) and the HE of imidacloprid (dark blue) (see Figure 4A) is plotted. For those genes, which are also DEGs after exposure to the LE of imidacloprid, the corresponding lfc is shown (light blue). **(B)** as in (A), but for the common subset of DEGs after exposure to the HE of fipronil (orange) and the LE of imidacloprid (light blue) (see Figure 4A).

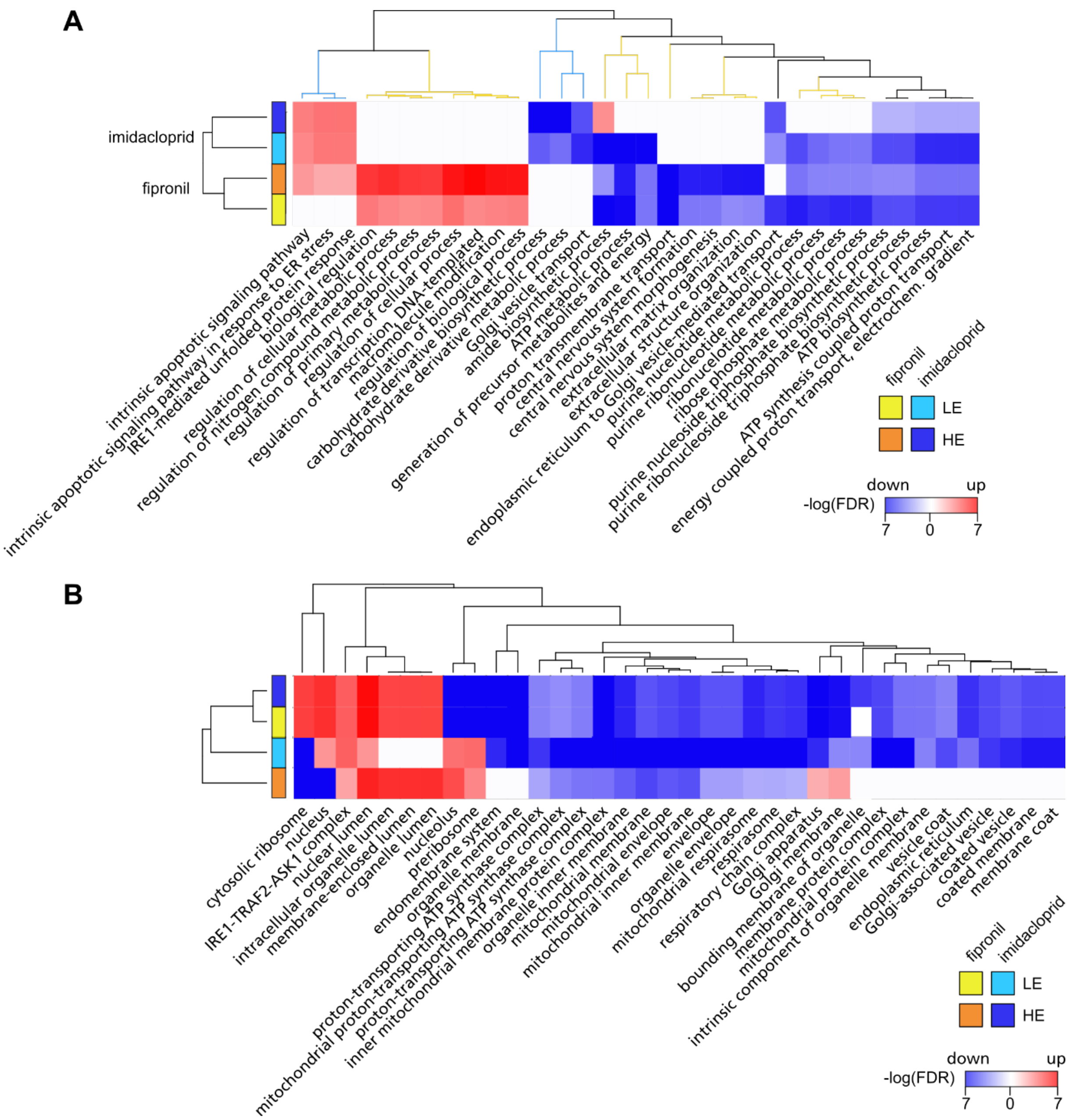

Figure S 7: GSE analysis after exposure to fipronil and imidacloprid based on the log2-fold change values. **(A)** Heatmap of gene ontologies (biological process) statistically significantly (FDR ≤ 0.01) enriched in the low and high exposure condition of each substance as identified by gene set enrichment analysis. –log(FDR) values are displayed as a color code. Up-regulation is indicated in red and down-regulation is indicated in blue. Non-significant as well as no regulation is colored in white. Gene ontologies and conditions are clustered by Euclidean distance based on the –log(FDR) change values. Clusters are colored by test substance as applied for signatures in panel B of Figure 4. **(B)** as in (A), but for cellular components statistically significantly (FDR ≤ 0.01) enriched in the low and high exposure condition. –log(FDR) values are displayed as a color code.

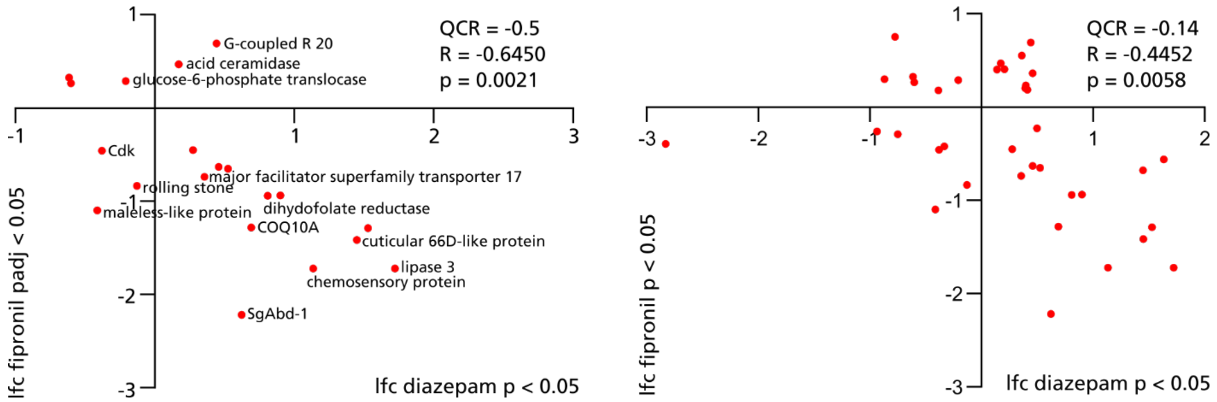

Figure S 8: Comparison of fipronil results with results obtained in a previous study for diazepam by Fuertes et al. (Fuertes et al. 2019). For the assigned set of DEGs (either padj ≤ 0.05 (left) or p ≤ 0.05 (right)) after fipronil exposure to HE, those genes with a statistically significant ($p \leq 0.05$) differential expression after exposure to diazepam are shown in a scatter plot. Log_2-fold change (lfc) values after exposure to diazepam are plotted on the x-axis and lfc values after fipronil exposure are plotted on the y-axis. Gene names are given for all annotated genes. The quadrant count ratio (QCR), the Pearson correlation coefficient (R) as well as the corresponding p-value is indicated.

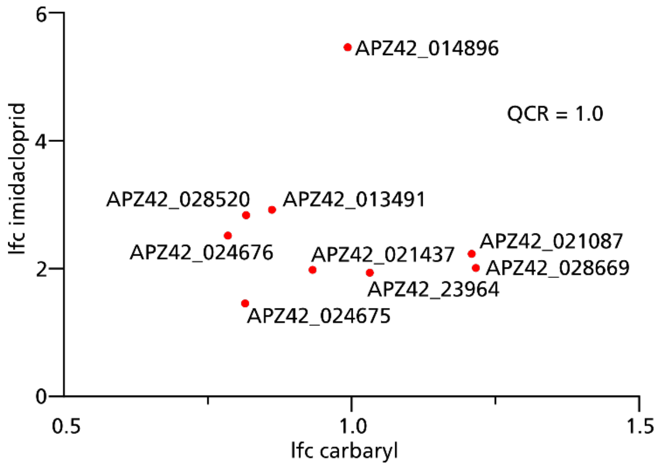

Figure S 9: Comparison of imidacloprid results with results obtained in a previous study for carbaryl by Orsini et al. (Orsini et al. 2016). For the assigned set of DEGs after imidacloprid exposure to HE, those genes with a statistically significant (padj ≤ 0.05) differential expression after exposure to carbaryl are shown in a scatter plot. Log_2-fold change (lfc) values after exposure to carbaryl are plotted on the x-axis and lfc values after imidacloprid exposure are plotted on the y-axis. Gene IDs are given for all genes. The quadrant count ratio (QCR) is indicated.

Supplemental References

Andrews, S. FastQC: a quality control tool for high throughput sequence data. 2010;

Athar, A.; Fullgrabe, A.; George, N.; Iqbal, H.; Huerta, L.; Ali, A.; Snow, C.; Fonseca, N.A.; Petryszak, R.; Papatheodorou, I.; Sarkans, U.; Brazma, A. ArrayExpress update - from bulk to single-cell expression data. Nucleic Acids Res 2019;47:D711-D715

Bolger, A.M.; Lohse, M.; Usadel, B. Trimmomatic: a flexible trimmer for Illumina sequence data. Bioinformatics 2014;30:2114-2120

Dobin, A.; Davis, C.A.; Schlesinger, F.; Drenkow, J.; Zaleski, C.; Jha, S.; Batut, P.; Chaisson, M.; Gingeras, T.R. STAR: ultrafast universal RNA-seq aligner. Bioinformatics 2013;29:15-21

Fuertes, I.; Campos, B.; Rivetti, C.; Pina, B.; Barata, C. Effects of Single and Combined Low Concentrations of Neuroactive Drugs on Daphnia magna Reproduction and Transcriptomic Responses. Environ Sci Technol 2019;53:11979-11987

Ignatiadis, N.; Klaus, B.; Zaugg, J.B.; Huber, W. Data-driven hypothesis weighting increases detection power in genome-scale multiple testing. Nat Methods 2016;13:577-580

Liao, Y.; Smyth, G.K.; Shi, W. featureCounts: an efficient general purpose program for assigning sequence reads to genomic features. Bioinformatics 2014;30:923-930

Loraine, A.E.; Blakley, I.C.; Jagadeesan, S.; Harper, J.; Miller, G.; Firon, N. Analysis and visualization of RNA-Seq expression data using RStudio, Bioconductor, and Integrated Genome Browser. Methods Mol Biol 2015;1284:481-501

Love, M.I.; Huber, W.; Anders, S. Moderated estimation of fold change and dispersion for RNA-seq data with DESeq2. Genome Biol 2014;15:550

Orsini, L.; Gilbert, D.; Podicheti, R.; Jansen, M.; Brown, J.B.; Solari, O.S.; Spanier, K.I.; Colbourne, J.K.; Rush, D.; Decaestecker, E.; Asselman, J.; De Schamphelaere, K.A.C.; Ebert, D.; Haag, C.R.; Kvist, J.; Laforsch, C.; Petrusek, A.; Beckerman, A.P.; Little, T.J.; Chaturvedi, A.; Pfrender, M.E.; De Meester, L.; Frilander, M.J. Daphnia magna transcriptome by RNA-Seq across 12 environmental stressors. Sci Data 2016;3

R Core Team. R: A Language and Environment for Statistical Computing. ed^eds. Vienna, Austria; 2019

Zhu, A.; Ibrahim, J.G.; Love, M.I. Heavy-tailed prior distributions for sequence count data: removing the noise and preserving large differences. Bioinformatics 2019;35:2084-2092